A Comprehensive P-Q Capability Study for Grid Interconnection of Inverter Based Resources Plant

Shahinur Rahman, Shuhui Li, Himadry Shekhar Das
Electrical and Computer Engineering Department
The University of Alabama, Tuscaloosa
Email: srahman6@crimson.ua.edu, sli@eng.ua.edu, hdas@crimson.ua.edu

***Abstract*—With the increased inverter-based resources (IBR connected to the grid, IBR P-Q capability charts are need proposed, and developed by the power industry to assure I operation efficiency and reliability. This paper presents a co prehensive P-Q capability evaluation for an IBR plant interc nected with the transmission grid. The proposed study consid the impact of different IBR grid-connected filters, IBR vec control implementation in the dq reference frame, and spe interconnection nature of IBRs in a plant structure. The mod and algorithms developed for the IBR P-Q capability analysis have considered specific IBR constraints that are different from those of a synchronous generator. The paper especially focuses on exploring the P-Q capability characteristics of IBRs and IBR plant at different interconnection points that are important for managing, designing, and controlling IBRs within an IBR plant, and for the development of international standards, such as IEEE P2800, for connecting IBRs to the transmission and distribution grids in a plant structure.**

***Index Terms*—Inverter-based resources, P-Q capability charts, vector control, grid-connected filters.**

I. Introduction

The worldwide acceptance of renewable energy resources such as solar and wind has led to the emergence of a new set of generators. These resources are either completely or partially connected to the grid through power electronic inverters, hence referred to as inverter-based resources (IBRs) [1]. Not long ago, the development of solar and wind farms was typically driven by small regional players, and the cost was significantly higher than that of a coal plant. Today, the cost of renewables has significantly plummeted, many solar and wind projects are undertaken by large multinational companies, and the scale of the solar and wind farms has also reached from MW scale around the year 2000 to GW scale now. This trend of growth has driven the rapid development of a new IEEE standard, IEEE Std. 2800-2022 [2], which focuses on IBR interconnection to the transmission and distribution grid in plant structures.

Nowadays, an IBR plant, such as a wind or solar photovoltaic power plant, could consist of hundreds to thousands of MW-scale wind turbines or MW-scale PV arrays to generate a large amount of power. Traditionally, for a synchronous generator, a boundary within which the machine can operate safely is defined via the P-Q Capability Curve and is used to guide the control of the generator [3], [4]. Similarly, the IBR P-Q capability is becoming one of the most important specifications of international standards [2], [5]. Various IBR P-Q capability charts have been developed. The NERC (North America Electric Reliability Corp.) Reliability Guideline in [6] presented a near semi-circle P-Q capability curve for nominal voltage with fixed reactive capability at around 0.95 p.u. active power output levels (Fig. 1a). The Electric Reliability Council of Texas (ERCOT) presented a D-shape P-Q capability curve (Fig. 1b) that needs to meet at the Point of Interconnection (POI) [7]. IEEE Std. 2800-2022 specifies a P-Q capability chart (Fig. 1c) that is similar to ERCOT's P-Q capability chart except the maximum reactive power injection/absorption limit. However, an IBR has a highly complex control system that is different from a synchronous generator. Also, the IBR operation is constrained by several factors, some of which are similar to the synchronous generator while others are quite different. In addition, for IBR interconnection to the grid in a plant structure, there is a need for a detailed P-Q capability characteristic study at different interconnection points in order to ensure proper operation of IBRs withing a plant and IBR plant and grid integration. All these factors affect the safe and reliable operation of IBRs within a plant. These issues need to be addressed to enhance the development of international standards as more and more IBRs are interconnected to the grid in plant configurations.

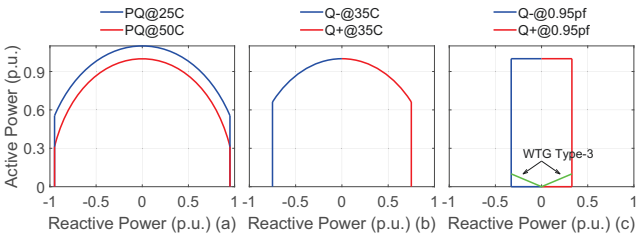

Fig. 1: P-Q capability charts provided by (a) NERC [6] and (b) ERCOT [7], and (c) IEEE Std. 2800 [2].

So far, no research has been found in the literature that explores the dynamic P-Q capability from the IBR-grid interconnection perspective in an IBR plant configuration. Therefore, this paper focuses on investigating dynamic P-Q capability of IBRs considering characteristics and constraints that are unique from the IBR-grid integration perspectives, especially in a plant structure. Overall, the results of this paper may guide the power community to identify the root cause of many abnormalities associated with grid-connected IBR plants, and help legislators to improve the industry guidelines and introduce new control methods (e.g. a neural network

2023 IEEE Industry Applications Society Annual Meeting (IAS) | 979-8-3503-2016-9/23/$31.00 ©2023 IEEE | DOI: 10.1109/IAS54024.2023.10406385

based vector controller [8]). Based on this pathway, the main contributions of this paper are as follows:

1) Active and reactive power models of a grid-tied IBR unit and IBR plant are developed by considering IBR control in the dq reference frame.

2) Algorithms are developed to explore the dynamic PQ capability characteristics from a grid-tied IBR unit to an IBR plant by considering constraints that are unique from IBR-grid integration perspectives.

3) Dynamic P-Q capability charts from a grid-tied IBR unit to an IBR plant are studied at different grid interconnection points.

The rest of the paper is structured as follows. Output power model of a grid-tied IBR and algorithms to determine P-Q capability charts are presented in Section II. Section III presents a study of P-Q capability characteristics of an individual IBR at different interconnection points. Section IV develops the output power model and theoretical P-Q capability study for multiple IBRs connected to the transmission grid in a plant structure. Section V presents a P-Q capability study for the IBR plant at different interconnection points as the number of IBRs added to the plant increases/decreases. Finally, the paper concludes with summary remarks.

II. Determine P-Q Capability of a Grid-Tied IBR at Different Interconnection Points

A. Output power model of a grid-tied IBR

IBRs are typically connected to the grid through an interconnection system as shown in Fig. 2a. The point where an IBR unit is electrically connected to a collector system refers to as the point of connection (PCC), the point between the high voltage bus of the IBRs and the interconnection system refers to as the point of measurement (POM), and the point where the interconnection system connects an IBR to the transmission system refers to as the point of interconnection (POI). An IBR is generally connected at the PCC through a grid-connected filter. The three typical grid filters are L, LC and LCL filters. The IBR output power to the grid can be evaluated at the PCC, POM and POI.

Without losing generality, the output power model development of an L-filter IBR is presented below. Fig. 2b shows the schematic of an IBR with an L-filter, in which R_f and L_f are the resistance and inductance of the L-filter inductor. R_{l1} and L_{l1} represent the resistance and inductance between the PCC and POM, and R_{l2} and L_{l2} represent the resistance and inductance of the interconnection system between the POM and POI. In the dq reference frame [9], the voltage balance equation of the L-filter inductor is

$$v_{dq\_inv} = R_f i_{dq} + L_f \frac{di_{dq}}{dt} + j\omega_s L_f i_{dq} + v_{dq\_PCC} \quad (1)$$

The voltage balance equations between the POM and PCC and between the POI and POM are (2) and (3), respectively,

$$v_{dq\_PCC} = R_{l1} i_{dq} + L_{l1} \frac{di_{dq}}{dt} + j\omega_s L_{l1} i_{dq} + v_{dq\_POM} \quad (2)$$

$$v_{dq\_POM} = R_{l2} i_{dq} + L_{l2} \frac{di_{dq}}{dt} + j\omega_s L_{l2} i_{dq} + v_{dq\_POI} \quad (3)$$

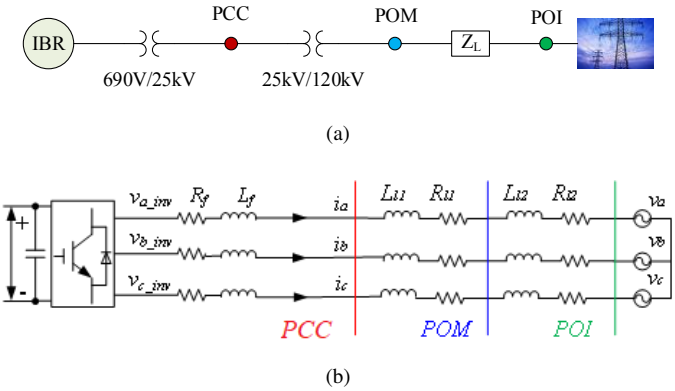

Fig. 2: Connecting IBRs to the transmission grid. (a) IBR interconnection via an interconnection system and (b) L-filter-based grid-connected IBR schematic.

where v_{dq_inv} represents the inverter terminal voltage, i_{dq} is the current flowing through the L-filter into the grid at the PCC, and v_{dq_PCC}, v_{dq_POM} and v_{dq_POI} are the PCC, POM, and POI voltages, respectively. In the steady-state condition, (1) - (3) become (4) - (6) as

$$V_{dq\_inv} = R_f I_{dq} + j\omega_s L_f I_{dq} + V_{dq\_PCC} \quad (4)$$

$$V_{dq\_PCC} = R_{l1} I_{dq} + j\omega_s L_{l1} I_{dq} + V_{dq\_POM} \quad (5)$$

$$V_{dq\_POM} = R_{l2} I_{dq} + j\omega_s L_{l2} I_{dq} + V_{dq\_POI} \quad (6)$$

where V_{dq_inv}, I_{dq}, V_{dq_PCC}, V_{dq_POM} and V_{dq_POI} denote the steady-state dq vectors of inverter output voltage, current in the L-filter, and PCC, POM and POI voltages. Thus, the complex power flowing from the IBR to the grid at the PCC, POM, and POI can be achieved as

$$P_{PCC} + jQ_{PCC} = V_{dq\_PCC} I^*_{dq} \quad (7)$$

$$P_{POM} + jQ_{POM} = V_{dq\_POM} I^*_{dq} \quad (8)$$

$$P_{POI} + jQ_{POI} = V_{dq\_POI} I^*_{dq} \quad (9)$$

Similarly, output power model of an IBR with an LC or LCL filter can be developed.

B. Algorithms to determine IBR P-Q capability charts

The IBR P-Q capability region represents the permissible output power region considering the physical constraints of the IBR, i.e., 1) rated power/current constraint and 2) PWM saturation constraint.

Firstly, an IBR is very sensitive to current. The rated current constraint requires that the magnitude of IBR dq current should be less than the rated dq current as follows

$$\sqrt{(I^*_d)^2 + (I^*_q)^2} \leq I_{rated} \quad (10)$$

Based on (10), the P-Q capability curve considering the IBR rated current constraint is determined as follows: (i) pick the voltage reference V^*_{dq} (1 p.u.) at PCC, POM, or POI, (ii) start with an IBR dq current I^*_{dq} whose magnitude equals to the rated current I_{rated}, (iii) calculate the voltage at the PCC,

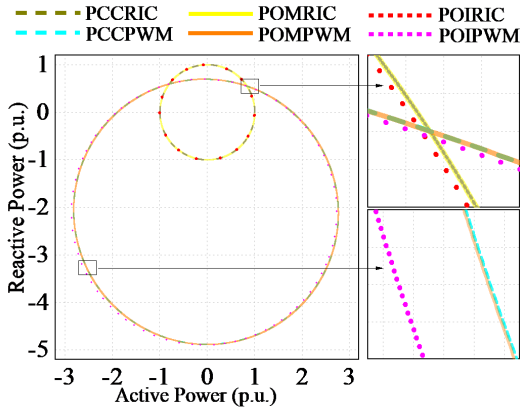

Fig. 3: P-Q capability charts of an IBR unit (considering POI as the reference).

POM, or POI based on (4) - (6), (iv) calculate the active and reactive power at the PCC, POM, or POI based on (7)-(9) and store the results, (v) get another rated IBR current I^*_{dq} and repeat (iii) to (v). The process continues till all the rated IBR current samples are swept once and then draw the P-Q capability curve at the PCC, POM, or POI.

Secondly, besides the rated current constraint, the output power of an IBR is also limited by the PWM saturation constraint [10]. This paper mainly focuses on sinusoidal PWM (SPWM) that is widely used in IBRs. Overall, the IBR d- and q-axis voltages, v_{d_inv} and v_{q_inv}, at the inverter output terminal should satisfy the following equation:

$$\sqrt{(v^*_{d\_inv})^2 + (v^*_{q\_inv})^2} \leq V_{dq\_max} \tag{11}$$

where V_{dq_max} is the maximum allowable inverter output terminal voltage calculated for SPWM [10], [11]. Thus, the algorithm to determine the P-Q capability chart considering the PWM saturation constraint involves the following steps: (i) pick the voltage reference V^*_{dq} (1 p.u.) at PCC, POM, or POI, (ii) start with an IBR dq output voltage V_{dq_inv} whose magnitude equals to V_{dq_max}; (iii) calculate I_{dq} based on (4) - (6); (iv) calculate the active/reactive power at the PCC, POM, or POI based on (7)-(9) and store the results; (v) repeat (ii) to (iv) for other dq output voltages whose magnitude equals to V_{dq_max}. The process continues till all the V_{dq_inv} samples, whose magnitude equals to V_{dq_max}, are swept once and then draw the P-Q capability charts at the PCC, POM, or POI.

III. P-Q Capability Analysis of a Grid-Tied IBR

The following parameters are used as the nominal values of an IBR unit. 1) The rated power is 1.5MVA. 2) The dc-link voltage is 1500V. 3) The grid-connected filter parameters are as follows: For the L filter, the inductance is 0.4mH and the resistance of the inductor is 0.003Ω. For the LC filter, the inductor remains the same, and the capacitance is 25μF. For the LCL filter, the capacitance remains unchanged while the inductance is 0.2mH and the resistance of the inductor is 0.0015Ω for both the inverter- and grid-side inductors. 4) The nominal grid line voltage referred to the PCC is 690V rms. The IBR unit is connected to a 690V/25kV step-up transformer (Fig. 2a). 5) The grid line voltage is 120kV, which is connected to the IBR via a transmission line and a 120kV/25kV step-down transformer. 6) The CSCR of the interconnection system is 2.5 that is calculated based on the maximum capacity of the IBR plant (600 1.5MW IBR units).

We evaluated the IBR P-Q capability at the PCC, POM, and POI using two different reference points, i.e., from the IBR perspective by taking PCC as the reference and from the grid interconnection perspective by taking POI as the reference. Fig. 3 shows the evaluation by taking POI as the reference. In general, the P-Q capability for the IBR with L, LC, and LCL filters are almost the same. Also, considering just one IBR in the transmission system, the difference between the P-Q capability obtained by using the PCC and POI as the reference point is very small. Fig. 3 shows the P-Q capability at the PCC, POM, and POI by taking POI as the reference, in which the circles with the center at the point [0, 0] represents the IBR rated current circle (RIC) while the other circles signify the IBR PWM saturation constraint circles. The P-Q capability region is the area enclosed by both the RIC and the PWM saturation constraint circle. As shown in Fig. 3, when just one IBR is considered, the P-Q capability regions looking at the PCC, POM, and POI are almost the same and is different from that of a synchronous generator and from the existing IBR P-Q capability charts used in the industry [6], [7], [12].

IV. Determine P-Q Capability of an IBR Plant at Different Interconnection Points

A. Output Power Model of an IBR Plant

An IBR plant is a group of IBRs in the same location connected together to produce electricity. Utility-scale wind and solar PV power plants with hundreds of megawatts have been built worldwide. If omitting the impedance of the collector system, a generalized grid-connected IBR plant can be shown in Fig. 4a and the equivalent circuit is shown in Fig. 4b in which all the IBRs have the same PCC voltage.

Without losing generality, let's assume all the IBRs have the same parameters. Then, the steady-state equations of each individual IBR j (j=1, …, N) can be obtained from (4) as

$$V_{dq\_inv,j} = R_f I_{dq,j} + j\omega_s L_f I_{dq,j} + V_{dq\_PCC} \tag{12}$$

The voltage balance equations between the POM and PCC and between the POI and POM are (13) and (14), respectively,

$$V_{dq\_PCC} = R_{l1} \sum_{j=1}^{N} I_{dq,j} + j\omega_s L_{l1} \sum_{j=1}^{N} I_{dq,j} + V_{dq\_POM} \tag{13}$$

$$V_{dq\_POM} = R_{l2} \sum_{j=1}^{N} I_{dq,j} + j\omega_s L_{l2} \sum_{j=1}^{N} I_{dq,j} + V_{dq\_POI} \tag{14}$$

For all IBRs, (12) can be written as

$$\sum_{j=1}^{N} V_{dq\_inv,j} = R_f \sum_{j=1}^{N} I_{dq,j} + j\omega_s L_f \sum_{j=1}^{N} I_{dq,j} + N V_{dq\_PCC} \tag{15}$$

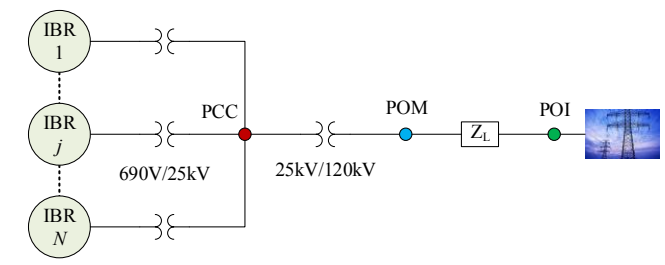

(a)

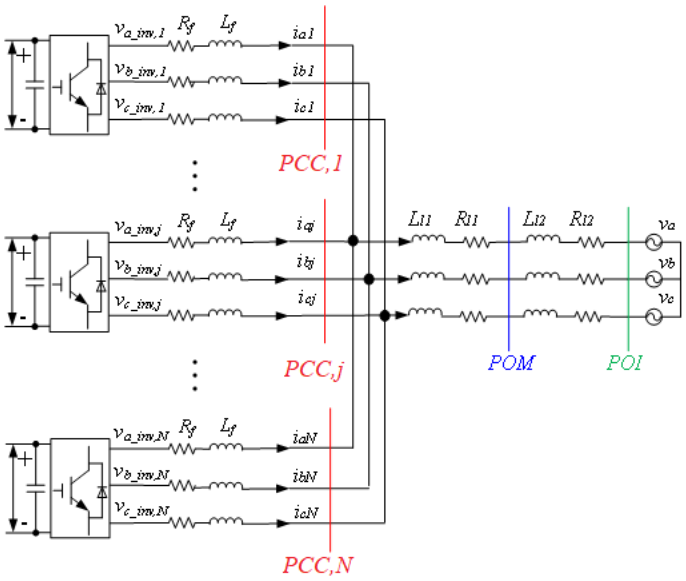

(b)

Fig. 4: A generalized grid connected IBR plant. (a) IBR plant schematic and (b) IBR plant equivalent circuit.

Assume that the grid current is I_{dq}. From Fig. 4b, we have $I_{dq} = \sum_{j=1}^{N} I_{dq,j}$. Rewrite (15), (13), and (14) as

$$\frac{1}{N}\sum_{j=1}^{N} V_{dq\_inv,j} = \frac{R_f}{N}\sum_{j=1}^{N} I_{dq,j} + j\omega_s \frac{L_f}{N}\sum_{j=1}^{N} I_{dq,j} + V_{dq\_PCC} \tag{16}$$

$$V_{dq\_PCC} = R_{l1} I_{dq} + j\omega_s L_{l1} I_{dq} + V_{dq\_POM} \tag{17}$$

$$V_{dq\_POM} = R_{l2} I_{dq} + j\omega_s L_{l2} I_{dq} + V_{dq\_POI} \tag{18}$$

From (16)-(18), the grid equivalent circuit of an IBR plant with N IBRs is similar to Fig. 5, where the equivalent circuit can be considered as an IBR plant being connected to the grid via a virtually variable grid-filter impedance that is equivalent to the parallel filter impedance of N IBRs connected online within an IBR plant. The IBR plant output voltage is the average of all N IBR output voltages and the IBR plant output current is the sum of all the IBR output currents. Then, based on Fig. 5 and algorithms developed in Section II.B, the IBR plant power at the PCC, POM, and POI can be obtained.

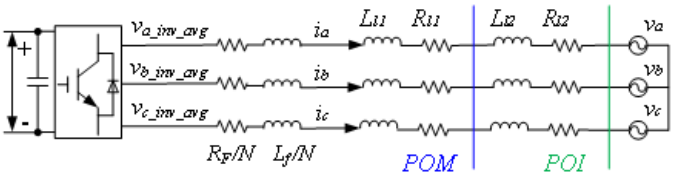

Fig. 5: Equivalent circuit of an IBR plant looking from the grid at the POM and POI.

B. Theoretical study of IBR plant P-Q capability

The plant P-Q capability at the POI, POM, and PCC should be obtained by considering 1) rated current and 2) PWM saturation constraints of IBRs within an IBR plant. We assume that all the IBRs within the plant have the same rating. Let's first define the IBR plant output power capability at the POI, POM, and PCC corresponding to the rated current and PWM saturation constraints of IBRs within an IBR plant.

Definition 1. The output power capability of an IBR plant at the IBR rated current condition represents the output power of the plant when the plant outputs the maximum current to the grid as all the IBRs within the plant operate at the rated current condition.

It is needed to determine how the maximum current passing through POM and POI is related to the rated current constraints of a group of IBRs that are tied to the PCC as shown in Fig. 4 which is proved below through Theorems 1 and 2.

Theorem 1. The maximum current passing through the POM and POI for two parallel IBRs tied together at the PCC can be obtained when both IBRs have their rated current amplitudes and the same angle.

Proof: Assume the current injected to the grid by the two parallel IBRs are I_{dq1} and I_{dq2} with angle of θ_1 and θ_2, respectively. Then, the resultant current flowing through POM and POI is

$$\begin{aligned} I_{dq} &= I_{dq1} + I_{dq2} \\ &= |I_{dq1}|\cos\theta_1 + j|I_{dq1}|\sin\theta_1 + |I_{dq2}|\cos\theta_2 + j|I_{dq2}|\sin\theta_2 \end{aligned} \tag{19}$$

From (19), the amplitude of the current passing through POM and POI is

$$|I_{dq}| = \sqrt{|I_{dq1}|^2 + |I_{dq2}|^2 + 2|I_{dq1}||I_{dq2}|\cos(\theta_1 - \theta_2)} \tag{20}$$

from which the maximum amplitude of I_{dq} appear when $\theta_1 = \theta_2 = \theta$, $I_{dq1} = I_{rated1}$ and $I_{dq2} = I_{rated2}$ and is

$$|I_{dq\_max}| = |I_{rated1}| + |I_{rated2}| \tag{21}$$

Thus, the maximum resultant current flowing through POM and POI can be expressed as

$$I_{dq\_max} = (I_{rated1} + I_{rated2})\angle\theta \tag{22}$$

Theorem 2. The maximum current passing through the POM and POI for N parallel IBRs tied together at the PCC can be obtained when all IBRs have their rated current amplitudes and the same rotating angle in the dq reference frame.

Proof. If N=2, the proof has been obtained as shown in Theorem 1.

Let's assume Theorem 2 is correct for N-1 IBRs tied together in parallel, i.e.,

$$I_{dq\_max} = (\sum_{k=1}^{N-1} I_{rated,k})\angle\theta \tag{23}$$

Then, for N IBRs tied together in parallel, the following can be obtained by applying Theorem 1 and (23) as

$$\begin{aligned} I_{dq\_max} &= (\sum_{k=1}^{N-1} I_{rated,k})\angle\theta + I_{rated,N}\angle\theta \\ &= (\sum_{k=1}^{N} I_{rated,k})\angle\theta \end{aligned} \tag{24}$$

Based on the Definition 1 and Theorem 2, we have

Lemma 1. The maximum output power capability of an IBR plant at the IBR rated current condition is the output power of the plant when each IBR within the plant outputs the rated current to the grid and has the same rotating angle.

Definition 2. The output power capability of an IBR plant at the IBR PWM saturation constraint condition represents the output power of the plant when the plant outputs the maximum voltage to the grid as all the IBRs within the plant operate at the PWM saturation limitation boundary.

Theorem 3. The maximum output voltage of an IBR plant for computing the output power capability of the plant can be obtained when all IBRs have the amplitudes of the output voltages at their PWM saturation boundary and all have the same angle.

Proof: According to Section IV.A, we get (25) for the j^{th} IBR

$$V_{dq\_inv,j} = Z_f I_{dq,j} + V_{dq\_PCC} \tag{25}$$

where Z_f stands for the L filter impedance. For the IBRs within the plant, we have

$$\begin{aligned} \sum_{j=1}^{N} V_{dq\_inv,j} &= Z_f \sum_{j=1}^{N} I_{dq,j} + NV_{dq\_PCC} \\ &= Z_f I_{dq} + NV_{dq\_PCC} \end{aligned} \tag{26}$$

From (26), the output current at the PCC is

$$I_{dq} = \frac{\frac{1}{N}\sum_{j=1}^{N} V_{dq\_inv,j} - V_{dq\_PCC}}{Z_f/N} \tag{27}$$

which means that the plant equivalent output voltage is $\sum_{j=1}^{N} V_{dq\_inv,j}/N$ and the plant equivalent impedance is Z_f/N. Based on Theorem 2, the plant outputs the maximum voltage when all the IBRs within the plant reach their PWM saturation limits and have the same angle.

Lemma 2. The maximum output power capability of an IBR plant at the IBR PWM saturation constraint boundary is the output power of the plant when each IBR within the plant outputs the PWM saturation voltage to the grid and has the same rotating angle.

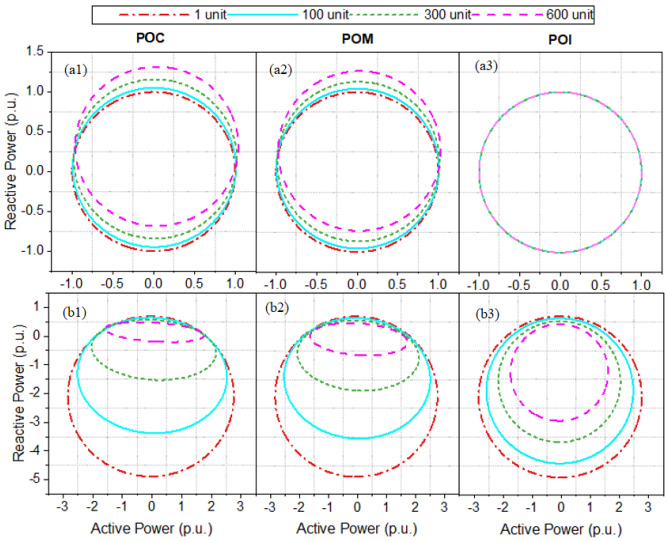

Fig. 6: IBR plant P-Q capability charts at the PCC, POM and POI when taking the POI as the reference: a1), a2), a3) P-Q capability charts corresponding to IBR rated current,; b1), b2), b3) P-Q capability charts corresponding to IBR PWM saturation constraint.

V. P-Q Capability Analysis of an IBR Plant

Based on the theorems and lemmas developed in Section IV, IBR plant P-Q capability charts at the PCC, POM, and POI are investigated in this section. The same IBR parameters used in Section II-B are utilized in this section for the evaluation. The P-Q capability study is divided into two parts, i.e., with and without the consideration of the collector system impact.

A. Without consideration of collector system impact

When neglecting the collector system impact, the IBR plant P-Q capability corresponding to the rated current and PWM saturation constraint conditions for the plant are determined based on Lemmas 1 and 2, respectively, in which the number of the IBR units connected online changes from 1 to 600.

Fig. 6 shows the plant P-Q capability evaluation by taking POI as the reference. The figure shows that with the increase of the number of IBR units connected online, the difference of the plant P-Q capability at the PCC, POM, and POI becomes evident. This would have an important impact on the control of individual IBRs within the plant. Typically, the power control of an IBR plant at the POI or POM is translated to power control commands that are distributed to each individual IBR. The task of each IBR unit is to follow the reference power commands from the plant level controller. Based on Figs. 6, the following remarks are obtained.

1) At the POI, the P-Q capability charts corresponding to the IBR rated current constraint remain the same (Fig. 6(a3)) while the P-Q capability charts corresponding to the IBR PWM saturation constraint (Fig. 6(b3)) shrinks as the number of the IBRs connected online increases. The reason of this is that for the same injected voltage of an IBR at the PWM saturation boundary, the PCC voltage increases when the current from more IBRs needs to pass through the interconnection

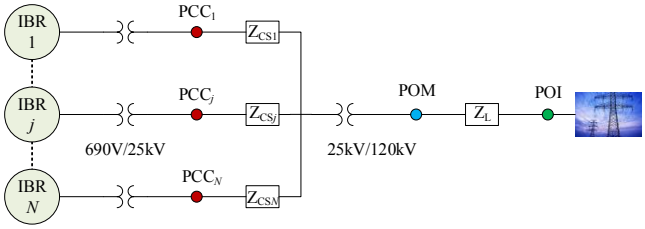

(a) IBR plant schematic with collector impedance.

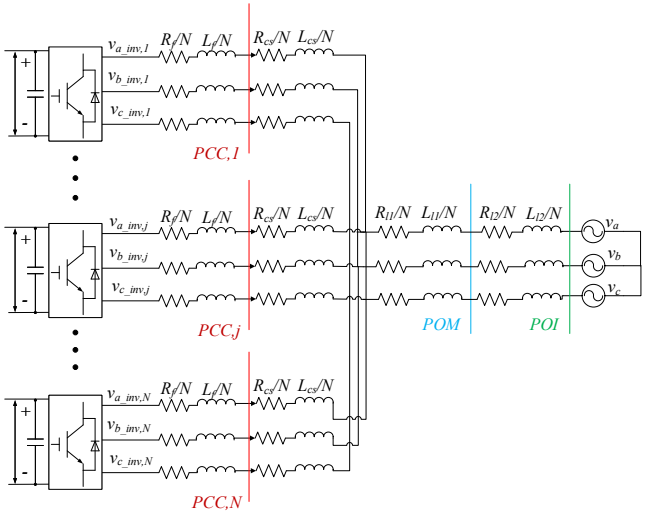

(b) IBR plant equivalent circuit with collector impedance.

Fig. 7: A generalized grid connected IBR plant with collector impedance.

system, causing the current that can be delivered by each IBR decreases. This makes the combined P-Q capability region smaller at the POI and the per unit power that the IBR plant can be delivered to the grid reduces as more IBRs are connected online within the IBR plant.

2) At the PCC, the P-Q capability charts corresponding to the IBR rated current constraint shifted up as the number of the IBRs connected online increases because more generating reactive power is needed due to the impedance of the interconnection system between the PCC and POI. On the other hand, the P-Q capability charts corresponding to the IBR PWM saturation constraint change from a circle to ellipse with much a smaller region as the number of IBRs connected online increases. The combination of the two makes the effective IBR P-Q capability region much smaller at the PCC and the per unit power that an IBR can be delivered to the grid reduce as more IBRs are connected online within the IBR plant.

3) From the plant control perspective, the reference power command presented to the IBR plant at the POI must consider change of the P-Q capability region to ensure the safe operation of the plant as the number of IBRs connected online increases according to Remark 1 obtained above.

4) From the control perspective of individual IBR, the reference power command presented to each IBR can be significantly affected when more IBRs are connected online according to Remark 2 obtained above. This factor must be considered properly. Otherwise, the safe and reliable operation of an IBR cannot be assured.

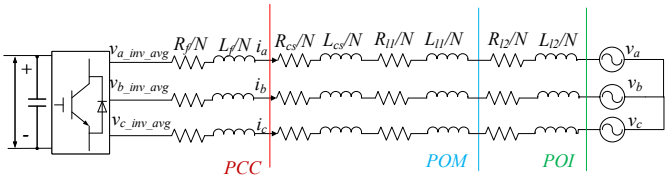

Fig. 8: Equivalent circuit of an IBR plant looking from the grid considering collector system impedance.

B. With consideration of collector system impact

When considering the impedance of the collector system, the plant P-Q capability study becomes more complicated. Without losing generality, a grid-connected IBR plant can be shown in Fig. 7a and the equivalent circuit is shown in Fig. 7b, in which each IBR will have a different PCC voltage. Assume all IBRs are connected to the POM via the same collector system impedance, R_{CS} and L_{CS}. Then, the voltage balance equation between the POM and PCC of each individual IBR j (j=1,....N) is as follows.

$$V_{dq\_PCC,j} = (R_{CS} + j\omega_s L_{CS})I_{dq,j} + (R_{l1} + j\omega_s L_{l1})I_{dq} + V_{dq\_POM} \tag{28}$$

Sum (28) for all IBRs, we have

$$\sum_{j=1}^{N} V_{dq\_PCC,j} = (R_{CS} + j\omega_s L_{CS}) \sum_{j=1}^{N} I_{dq,j} + (R_{l1} + j\omega_s L_{l1})NI_{dq} + NV_{dq\_POM} \tag{29}$$

Assume that the grid current is I_{dq}. From Fig. 7b, we have $I_{dq} = \sum_{j=1}^{N} I_{dq,j}$. Rewrite (29) as

$$\frac{1}{N}\sum_{j=1}^{N} V_{dq\_PCC,j} = (\frac{R_{CS}}{N} + j\omega_s \frac{L_{CS}}{N})I_{dq} + (R_{l1} + j\omega_s L_{l1})I_{dq} + V_{dq\_POM} \tag{30}$$

Then, from the grid perspective, the equivalent circuit of the IBR plant considering collector system impedance is obtained as shown in Fig. 8, where the plant can be considered as being connected to the grid via a virtually variable impedance that is the parallel of the filter and collector system impedance of N IBRs connected online within an IBR plant. The IBR plant output voltage is the average of all N IBR output voltages and the IBR plant output current is the sum of all the IBR output currents. The IBR plant PCC voltage is the average of all N IBR PCC voltages.

Note: the dynamic equations of each IBR and its L-filter are not presented here in developing the plant equivalent circuit of Fig. 8. For a general IBR plant, a more complicated plant equivalent circuit can be developed using the same development strategy.

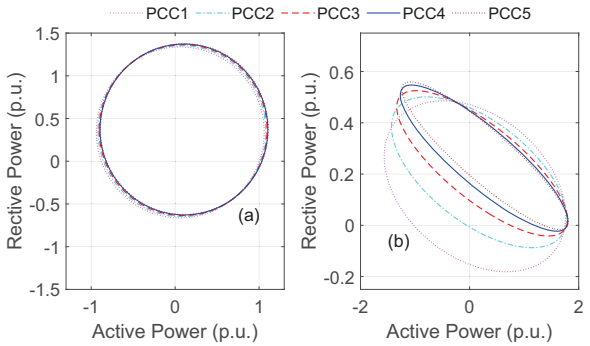

Fig. 9: P-Q capability (at PCC) of an IBR plant considering (a) Rated current boundary and (b) PWM saturation Limit.

Without losing generality, one representative IBR plant configuration is utilized here to demonstrate the plant P-Q capability study considering the collector system impact. The plant contains 5 clusters of wind turbines. Each cluster consists of 120 wind turbines and wind turbines in each cluster are tied together via the same collector impedance. Each cluster is connected to the POM via a different collector impedance.

As all the IBRs share the same POI and POM voltages, similar remarks can still be obtained for the IBR plant P-Q capability at the POI and POM, as shown in Fig. 6. However, at the PCC, it was found that each IBR shows different P-Q capability charts. Fig. 9 shows the P-Q capability study, by taking POI as the reference, at the PCC of wind turbines in each cluster. The figure shows that the P-Q capability charts at the PCC corresponding to the rated current constraint are close while the P-Q capability charts corresponding to the PWM saturation constraint shrinks as the collector system impedance connecting a cluster to the POM increases, which makes the effective P-Q capability region smaller at the PCC as the collector system impedance increases.

Overall, when considering the collector system impedance impact, the difference of the wind turbine P-Q capability at the PCC of wind turbines in each cluster also becomes evident because each cluster is connected to the POM via different collector system impedance. This factor, if not considered properly in the control of an IBR plant, can also affect the safe and reliable operation of IBRs in a plant.

VI. Conclusion

P-Q capability analysis of grid-connected IBRs in a plant structure is an important factor for the stable and reliable operation of the IBRs within that plant. This paper presents a comprehensive P-Q capability study for grid interconnection of an individual IBR and an IBR in plant configuration. The results show that IBR P-Q capability chart is quite different from that of a synchronous generator and from the traditional IBR P-Q capability charts used in the industry. The study indicates that the design and control of an IBR, such as grid-connected filter, converter constraints are important to determine IBR P-Q capability curve that can meet the grid interconnection requirements. The study also indicates that P-Q capability of IBRs in a plant structure is different. The results show that the number of IBRs in a plant connected online, collector system impedance, and grid interconnection locations could affect the actual physical IBR plant P-Q capability chart a lot and significantly shrink the permissible P-Q capability area, which would affect the safe operation of IBRs if this factor is not considered in presenting control commands to individual IBRs. The conventional IBR P-Q capability charts used in the industry could either cause the abnormal operation of an IBR or significant waste of the IBR P-Q capability resource. Thus, the power and energy community should come forward to develop new international standards for managing, designing, and controlling IBRs within an IBR plant.

References

[1] J. Matevosyan and J. MacDowell, "A future with inverter-based resources: Finding strength from traditional weakness," *IEEE Power Energy Mag.*, vol. 19, no. 6, pp. 18–28, Oct. 2021.

[2] IEEE std 2800 - standard for interconnection and interoperability of inverter-based resources interconnecting with associated transmission electric power systems. https://standards.ieee.org/project/2800.html.

[3] N. Nilsson and J. Mercurio, "Synchronous generator capability curve testing and evaluation," *IEEE Trans. Power Del.*, vol. 9, no. 1, pp. 414–424, Jan. 1994.

[4] M. Adibi and D. Milanicz, "Reactive capability limitation of synchronous machines," *IEEE Trans. Power Syst.*, vol. 9, no. 1, pp. 29–40, Feb. 1994.

[5] "IEEE standard for interconnection and interoperability of distributed energy resources with associated electric power systems interfaces," *IEEE Std 1547-2018*, pp. 1–138, Apr. 2018.

[6] Reliability guideline bps-connected inverter-based resource performance. https://www.nerc.com/comm/OC_ReliabilityGuidelines_DL/Inverter-Based_Resource_Performance_Guideline.pdf. North American Electric Reliability Corporation (NERC) [Online; accessed Sep-2018].

[7] Inverter-based resource (IBR) workshop. http://ercot.com/content/wcm/key_documents_lists/176763/ERCOT_IBR_Workshop_April_25_2019.pdf. Electric Reliability Council of Texas (ERCOT).

[8] X. Fu and S. Li, "Systems, methods and devices for vector control of induction machines using artificial neural networks," 2021.

[9] S. Li, T. Haskew, and L. Xu, "Conventional and novel control designs for direct driven pmsg wind turbines," *Electric Power System Research*, vol. 80, no. 3, pp. 328–338, Mar. 2010.

[10] K. Zhou and D. Wang, "Relationship between space-vector modulation and three-phase carrier-based pwm: a comprehensive analysis," *IEEE Trans. Ind. Electron.*, vol. 49, no. 1, pp. 186–196, Feb. 2002.

[11] N. Mohan, "Advanced electric drives – analysis, modeling and control using matlab/simulink," *John Wiley & Sons, ISBN 978-1-118-48548-4*, 2014.

[12] Reactive power interconnection requirements for pv and wind plants. SANDIA REPORT - SAND2012-1098, Sandia National Laboratories, Feb. 2012.